Prototype for Automatable, Dielectrophoretically-Accessed Intracellular Membrane–Potential Measurements by Metal Electrodes

Ulrich Terpitz,[1,2] Vladimir L. Sukhorukov,[2] and Dirk Zimmermann[1,3]

[1]Department of Biophysical Chemistry, Max Planck Institute of Biophysics, Frankfurt am Main, Germany.
[2]Department of Biotechnology and Biophysics, Julius Maximilians University Würzburg, Würzburg, Germany.
[3]Department of Biochemistry, Chemistry and Pharmacy, Johann Wolfgang Goethe University, Frankfurt am Main, Germany.

ABSTRACT

Functional access to membrane proteins, for example, ion channels, of individual cells is an important prerequisite in drug discovery studies. The highly sophisticated patch-clamp method is widely used for electrogenic membrane proteins, but is demanding for the operator, and its automation remains challenging. The dielectrophoretically-accessed, intracellular membrane–potential measurement (DAIMM) method is a new technique showing high potential for automation of electrophysiological data recording in the whole-cell configuration. A cell suspension is brought between a mm-scaled planar electrode and a μm-scaled tip electrode, placed opposite to each other. Due to the asymmetric electrode configuration, the application of alternating electric fields (1–5 MHz) provokes a dielectrophoretic force acting on the target cell. As a consequence, the cell is accelerated and pierced by the tip electrode, hence functioning as the internal (working) electrode. We used the light-gated cation channel Channelrhodopsin-2 as a reporter protein expressed in HEK293 cells to characterize the DAIMM method in comparison with the patch-clamp technique.

INTRODUCTION

A number of diseases, such as migraine, epilepsy, and deafness,[1,2] are caused by dysfunctions of ion channels. Consequently, the investigation of ion channels is of high importance for pharmaceutical and clinical research.[3,4] However, data acquisition regarding the effect of various drug candidates on ion channels by manual patch-clamp is relatively slow, allowing only a low throughput.[5,6] During the last years, this bottleneck led to the development of a number of automated patch-clamp systems[7–10] predominantly used for cellular screening along the drug value chain.[11] Both manual and automatic patch-clamp systems share—apart from systems using antibiotics for membrane perforation[12]—that the cytoplasm of the cell is substituted by a physiological solution.[13] The substitution of the cytoplasm, which often leads to run-down effects,[12] is obsolete in several automated systems based on metal microelectrodes, but they are not offering the information depth of the patch-clamp methods. The majority of these metal microelectrode arrays are designed to measure extracellular processes[14] or to stimulate nerve cells.[15,16] Intracellular techniques by means of invasive metal electrodes are only rarely found.[17,18]

In the present communication, we introduce an electrophysiological method based on metal microelectrodes: the dielectrophoretically-accessed intracellular membrane–potential measurement (DAIMM) method (*Fig. 1*). A cell suspended in a low-conducting medium is exposed to a strongly inhomogeneous electric field and accelerated by the positive dielectrophoretic force F_{DEP} in the direction of a metal microelectrode located in a disposable carrier. F_{DEP} is defined by

$$F_{DEP} = 2\pi r^3 \varepsilon_m \, \mathrm{Re}[f_{CM}] \nabla \overline{E}^2_{rms} \qquad (1)$$

where r is the radius of the cell, ε_m the permittivity of the surrounding medium, $\mathrm{Re}[f_{CM}]$ the real part of the Clausius-Mosotti-factor, and ∇ the nabla operator. For a detailed theoretical introduction to dielectrophoretic manipulation of cells, please consult published works by Dimitrov,[19] Jones,[20] and Zimmerman and Neil.[21] While hitting the electrode tip, the cell is penetrated and internally, electrically contacted. The cell penetration is subsequently followed by spontaneous membrane sealing in the electrode entry zone. Electrophysiological cellular measurements can be performed when a seal of high resistance is established between the cell membrane and the carrier matrix—similar to a conventional patch-clamp setup, where a solution-filled glass microelectrode is used to penetrate the plasma membrane.

The DAIMM technique is characterized by significant differences compared to the patch-clamp technique:

1. After penetration of the microelectrode, the cytoplasm is preserved, and it can be expected that the physiological processes will remain nearly unaffected. Thus, measurements are also conceivable for periods of several hours provided that the tip electrodes are slim, preventing severe damage on the cell, for example, by rupture of the cell membrane.

ABBREVIATIONS: AFM, atomic-force microscopy; DAIMM, dielectrophoretically-accessed intracellular membrane–potential measurement; DEP, dielectrophoresis; HEPES, 4-(2-hydroxyethyl)-1-piperazineethanesulfonic acid; PC, personal computer.

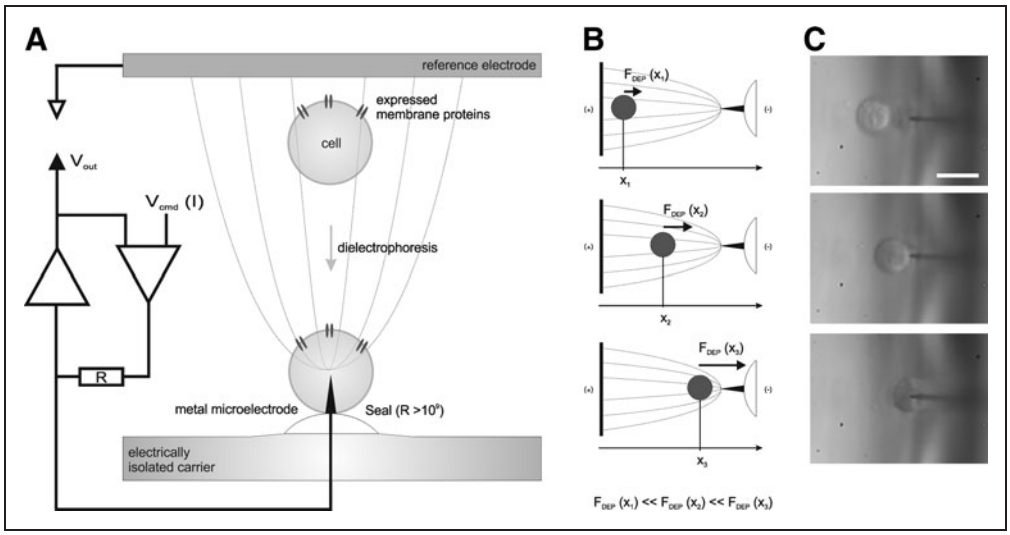

Fig. 1. The DAIMM method: **(A)** The measurement setup, the theoretical electric field lines, and the electronic circuit of the DAIMM method. Note that an important prerequisite is an asymmetric electrode configuration to establish inhomogeneous electric field conditions in the reaction compartment of the perfusion chamber. **(B)** The spatial gradient of dielectrophoretic forces on a manipulated single cell. These forces result in a movement of the manipulated cell toward the area of highest field (positive dielectrophoresis), that is, toward the tip of the smaller electrode of the asymmetric electrode configuration (single-spike electrode). Critical for establishing a cell configuration as shown in **(A)** is that the field parameters are selected in a way assuring that the single-spike electrode will penetrate the cell membrane without disruption of the cell. **(C)** Establishment of the system configuration depicted in **(A)** by using a HEK293 cell in a low-conductive medium (2 MHz, 30 V_{pp} alternating field, pulses of 300-ms duration). White scale bar = 10 μm. DAIMM, dielectrophoretically-accessed intracellular membrane-potential measurement.

2. Using the dielectrophoretic force for cell attraction allows electrophysiological measurements from cell suspensions with a very low density, as every viable cell positioned between the electrodes experiences a dielectric force.[21] Because of this sensitivity, dielectrophoresis (DEP) is used in many lab-on-the-chip applications.[22]
3. In voltage-clamp experiments, the high capacitance and strong polarization of the electrode (>100 μF/cm^2 at 10 Hz[23]) lead to a very high series resistance. Thus, the application of voltage-clamp is not feasible.

In contrast, under zero-current clamp conditions, changes of the membrane permeability by deactivation of ion channels are fast reported.

In this communication, we show a proof of principle for the new technique by using a lab model system and HEK293 cells expressing the light-activated cation channel Channelrhodopsin-2.[24] Changes of the membrane potential of HEK293 cells mediated in response to blue-light illumination were measured by use of the DAIMM methods.

MATERIALS AND METHODS

Microfluidic Chamber and DAIMM Setup

Dielectrophoretically controlled formation of the cell–electrode assembly was performed in a microfluidic measurement chamber (*Fig. 2A*). The main feature of this chamber consisted of a μm-scaled microelectrode (Ag/AgCl; single-spike electrode) mounted on a disposable carrier and a mm-scaled planar reference electrode (Ag/AgCl) located in opposite to the carrier in a distance of about 200 μm (*x*-axis). Both electrodes were connected to different peripheral devices via highly insulated input leads (TΩ-Range; see also the Carrier Design section) to apply electric fields for cell manipulation, and subsequently to record data from the electrode–cell array. Fluid channels with opening located next to the carrier (*y*-axis) allowed application/disposing of cells and solution exchange. The chamber volume was reduced to the smallest possible volume (about 50 μL) where no refraction of the optical pathway (*z*-axis) could take apart, and the quality of the microscopic image was satisfying.

A clear lid on top of the chamber prevented leakage of fluid during perfusion and allowed microscopic observation/filming of dielectrophoretic cell attraction. The whole microfluidic chamber was fixed on the cross table of a microscope (Axioskop; Zeiss) equipped with a high-velocity camera (Sensicam; PCO), installed on a vibration-attenuated table and protected by a faradic cage. Blue-light emission of a 50-W HBO lamp was controlled by a shutter (VS25 series/VCM-D1 driver; Vincent Associates). Note that the optical axis of the measurement chamber used for visual inspection of the experiment was only initially required to establish and optimize the workflow parameters, but automation of the workflow will make any visual inspection obsolete, thereby clearly reducing the complexity of the setup, assuming that other ion channels than the light-activated ChR2 will be expressed in routine use (*e.g.*, the pharmaceutical-relevant HERG cation channel).

Carrier Design

The carrier blank [poly(methyl methacrylate), 8 mm × 7 mm × 4 mm] contained three consecutive tubes (*Fig. 2B*). In the internal tube (1), the single-spike electrode was fixed by an UV adhesive, whereas the electric contact was located in the middle borehole (2). The large-scale borehole (3) mounted the input lead (a gold pin) with insulation.

Fine electrode tips were obtained by electrochemical etching (atomic force microscopy [AFM]–tip).[25,26] An Ag-bond wire (25-μm diameter; Heraeus) was mounted on a metal cantilever and brought for split seconds into an etching solution (20% perchloric acid in methanol)[25] located in a silver-wire loop (1-mm diameter; WPI) while a voltage of 1.5 V was applied. An inverse microscope

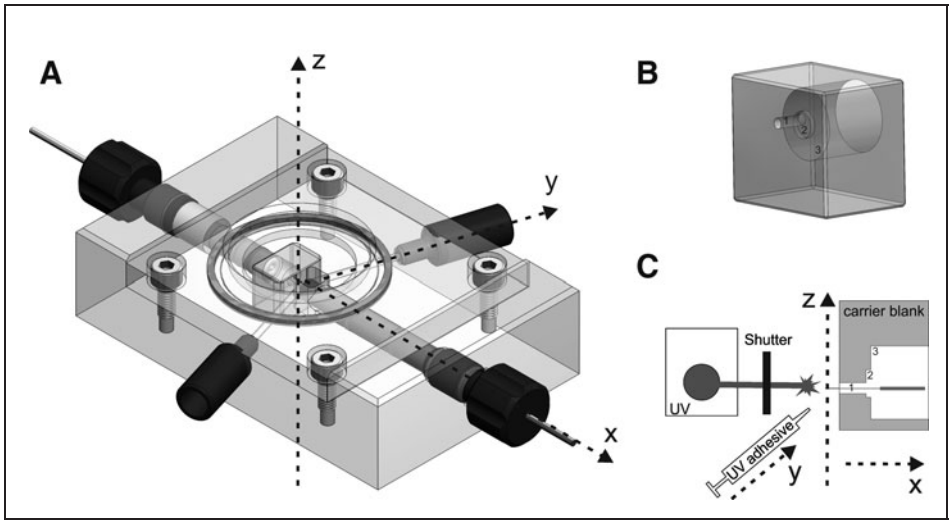

Fig. 2. Semiautomatic measurement setup for the DAIMM method. **(A)** The three-axis chamber (computer-aided design; Drawings 7.4, Dassault Systemes) is designed with the electronic circuit in the *x*-axis, the perfusion circuit in the *y*-axis, and an optical pathway in the *z*-axis. Note that the disposable carrier of the single-spike electrode is placed in the cross point of the three axis, and subsequently the chamber is sealed via a transparent glass lid. **(B)** Carrier blank. **(C)** The manufacturing process of a carrier with integrated single-spike electrode. A finely etched Ag-bond wire is threaded through the inner tube of the disposable carrier along the *x*-axis. Adhesive and subsequently ultraviolet light are applied under micromanipulator control using the *y*-axis. Visual control is given via the *z*-axis.

(Axiovert25; Zeiss) was used to control the fine tip and taper formation by a repolishing technique.[26] Etching procedure was repeated until a suitable tip form emerged (*Supplementary Fig. S1*; Supplementary Data are available online at www.liebertpub.com/adt). Note that a sharp tip and a slender taper are required for successful cell impalement by DAIMM. Subsequently, the etched silver tip was built into the chip carrier blank (*Fig. 2C*) under microscopic control by means of three micromanipulators installed on a vibration-attenuated table. The tip was threaded through the tubes of the blank and positioned in the middle of the little tube protruding ~300 µm. The UV adhesive (VL1605; Panacol) was filled into the little tube using a syringe needle (Microfil 34; WPI) until a convex shape was formed outside the chip. The tip length of the single-spike electrode was adjusted to 4–50 µm before the adhesive was hardened by UV illumination for 10 min. Thereafter, the silver wire was cut from the cantilever. The residue of the silver wire was coiled into the middle tube, and the tube was also filled with conductive silver (Busch GmbH), and a thin silver disk (200-µm section of a 1-mm silver wire) was set into the tube as the hindsight electric contact.

To exclude the occurrence of a short-circuit by leakage of the carrier matrix or electrode insulation, control chips were built. They either did not contain a silver wire, or the silver tip was covered with UV adhesive. When measured in physiological solutions, real resistances were higher than 1 TΩ (frequency < 1 Hz).

Reference Electrodes

A silver wire (1-mm diameter; WPI; elongated to 900 µm) was covered by the nonconducting electrode cylinder (*Fig. 2A*). The protruding front end was polished by means of a fine abrasive paper (P1200; Leco) to achieve a plan area in parallel to the chip surface. Please note that a parallel arrangement is very important for reproducible, dielectrophoretic experiments. The silver surface was chlorinated at 20–30 µA in 0.1normality HCl within 15 h.

Electronic Devices

Cells and liposomes were dielectrophoretically manipulated using alternating electric fields. According to *Equation (1)*, the cell was subjected to strong dielectrophoretic forces when the electric-field intensity becomes high, that is, in proximity with the single-spike electrode, and subsequently the cell was accelerated toward the microelectrode. To prevent destruction of the cell by the microelectrode during the membrane penetration process, an amplitude modulator was used to keep the forces applied to the cell under a threshold. The amplitude modulator reduces the amplitudes from 30 V_{pp} (generated by a function generator at 4 MHz; hp8116A; Hewlett Packard) down to 0 within a free eligible time between 0.2 and 1 s. Liposomes were dielectrophoretically manipulated at frequencies of up to 50 MHz without modulation. Cell membrane electroporation was achieved by a pulse generator (hp214B; Hewlett Packard).

The frequency-dependent resistance of the electrodes was measured by means of a potentiostat (Femtostat FAS1; Gamry) connected to a personal computer (PC). Data were recorded using software Framework V 4.35 (Gamry), and Echem Analyst 1.35 (Gamry) and Origin 7.5 (OriginLab Corporation) were used for data analysis. The single-spike microelectrode was set as a working electrode (applying the alternating field), whereas the reference and counter electrodes were connected to the AgCl reference electrode. The applied AC field ranged from 100 kHz to 1 Hz with amplitudes between 20 and 50 mV.

A patch-clamp amplifier (Axopatch 200B; Axon Instruments) connected to a PC by an analog/digital converter (DigiData 1200; Axon Instruments) was used for potential measurements. The single-spike electrode was plugged in the patch-pipette position of the headstage. Potential recordings were performed at zero current ($I = 0$). Data obtained by electrode recordings were low-pass filtered at 2 or 5 kHz and digitized at a sampling rate of 1–10 kHz using Clampex 9.1 (Axon). For data analysis, the software programs Clampfit 9.1 (Axon) and Origin 7.5 (OriginLab) were used.

Solutions

The measurement chamber was perfused by physiological solutions at a flow rate of up to 1 mL/min. If not stated otherwise, the solutions contained 100 mM NaCl, 2 mM $CaCl_2$, and 2 mM $MgCl_2$, and 10 mM 4-(2-hydroxyethyl)-1-piperazineethanesulfonic acid (HEPES), pH 7.4. Osmolarity was adjusted to 280 mOsm by addition of sorbitol. Dielectrophoretic attraction was performed in a low-conducting DEP-Medium, which contained 0.1 mM calcium acetate and 0.5 mM magnesium acetate and was adjusted to 200 mOsm by sorbitol. In some experiments, sorbitol was replaced by the same amount of Nycodenz© (Nycomed) to avoid sedimentation of cells (N-DEP Medium).

Characterization of Electrodes

Single-spike electrodes (0.1–1 nA, ~5 min) were chlorinated immediately before experiments in the measuring chamber in a physiological solution. Successful chlorination was proved by a significant drop of the resistance by at least a factor of 5 down to 2.2 ± 2.2 GΩ·μm^2 (at 10 Hz; $n = 52$). This value is similar to that of other silver microelectrodes (0.5 GΩ·μm^2)[27] and much lower than that of pure silver electrodes (38.2 GΩ·μm^2)[28]. The resistance was clearly frequency dependent (1 Hz → 11.97 ± 3.02 GΩ·μm^2; 100 Hz → 1.67 ± 0.63 GΩ·μm^2; $n = 8$). A typical impedance measurement (1–10^5 Hz) of a single-spike microelectrode before and after chlorination is shown in *Supplementary Figure S2*. Note that the area-specific resistance values were normalized to the theoretical electrode area, which was calculated for the lateral area assuming a cone form of the single spike (parameters were obtained from microscopic pictures). The variability of the area-specific electrodes can be explained by the fact that the real geometric form of the single-spike electrode often slightly differed from a cone. In addition, the effective electrode surface depends on the grade of chlorination, as silver chloride deposition leads to a surface enhancement.[28,29]

Chlorinated silver single spikes mounted at the carrier showed high potential stability (0.31 ± 0.32 mV/min, $n = 55$) in a physiological solution, but not in Cl^--deficient DEP solution. No significant changes in potential were observed after a pH change in the perfusing solution (pH 6–10). Indeed, a potential drift of > 0.5 mV/min was exclusively observed from electrodes with surfaces < 500 μm^2. Similarly, also a decrease of the area-specific electrode conductivity was associated with an increased drift. Both observations can probably be traced back to an insufficient chlorination.[28] Blue-light illumination of chlorinated silver single-spike electrodes (required for activation of the light-gated ion channel ChR2) evoked a slight light-dependent depolarization (1.02 ± 2.68 mV, $n = 16$).

The stability of electrodes during the cell manipulation process was tested. Electric fields necessary for dielectrophoretic cell manipulation were applied to pure electrodes in DEP solution for several minutes. Thereafter, in some cases, the resistance of the single-spike electrodes and also the drift within a subset of the electrodes was slightly increased, indicating the general robustness of the measurement system. No significant changes in electrode isolation were observed by applying the described regime.

Cell Attraction and Measurements

HEK293 and HEK293-ChR2-YFP cells were cultured as described before.[24] Cells were harvested by centrifugation (4 min, 400 *g*) and washed two times in DEP medium. Subsequently, cells were re-suspended in (N-)DEP medium (200 mOsm) to a density of about 10^5 cells/mL.

To establish low-electrolyte conditions in the measurement chamber, the microfluidic chamber was perfused for >10 min before performing experiments. Subsequently, a cell suspension was applied via the perfusion systems. The horizontal position (*y*-axis) of a single cell was controlled by syringes connected to the cell reservoir (hydraulic control). Single-cell DEP was performed at amplitude modulation time of 0.2–0.5 s and a voltage of 30 V_{pp} at 2.5–4.5 MHz, and documented by means of a high-velocity camera.

Alternatively, multi-cell attraction was performed without modulation at the same frequencies. When cells were located on the tip, electroporation of the cell membrane was reached by applying a series of four to five pulses with intensities of 40 V and 20–30-μs duration. Subsequently, a liposome suspension (see the Liposomes section) was applied to insulate the free electrode surfaces.

Liposomes

The single-spike electrode was electrically isolated by dielectrophoretic attraction of electrolyte containing liposomes suspended in a low-conducting medium. After attraction, development of a stable lipid phase on the free electrode surface is expected.[30] Ultrasonication (1 min) was used to suspend 20 mg 1,2-dioleoyl-sn-glycero-3-phosphocholine and 2 mg cholesterol in 5 mL liposome buffer (120 mM KCl, 10 mM HEPES, 5 mM ethylenediaminetetraacetic acid [EDTA], 50 mM Nycodenz©). Liposomes of 100-nm diameter were produced using Liposofast (Avestin). Liposomes were transferred into a liposome buffer without Nycodenz (1:5) and centrifuged (5 min, 4,500 *g*, 4°C). After two washing steps in DEP solution, the pellet was resuspended in 1 mL DEP solution. The DEP–liposome suspension was suitable for DEP up to 12 h. Electric-field frequency was set to 35–45 MHz, and an amplitude of 30 V_{pp} was used. The single-spike electrodes were completely loaded with liposomes 20 s after starting the electric field. This seal was mechanically stable, and the impedance of the electrode was clearly enlarged by two orders of magnitude.

Patch-Clamp Experiments

Light-dependent membrane–potential depolarization mediated by the light-activated ion channel Channelrhodopsin-2 was recorded using a patch-clamp setup described by Zimmerman *et al.*[24] The pipette solution consisted of 100 mM KCl, 20 mM KCl, 10 mM HEPES, and 5 mM EDTA. The bath solution contained 100 mM NaCl, 2 mM $CaCl_2$, 2 mM $MgCl_2$, and 10 mM HEPES. Both solutions were adjusted to 290 mOsm and pH 7.4 by sorbitol and HCl, respectively.

Measurements were performed in the current clamp mode at zero current.

RESULTS AND DISCUSSION

Cell Access

The feasibility of the DAIMM technique was proven by means of a handmade single-spike Ag/AgCl microelectrode chosen as a model system. Indeed, upon application of alternating electric fields in the one digit MHz range HEK293 cells (suspended in a low-conducting DEP medium) were strongly accelerated by the positive dielectrophoretic force F_{DEP} toward the single-spike electrode, and subsequently intracellularly contacted (*Fig. 1C*). To avoid adverse side effects during cell perforation, the cell was moved in small, successive steps by modulating the applied alternating field from maximal amplitude down to 0 mV within 0.2–0.3 s for every step. Nevertheless, the kinetic energy of the moving cell was still so high that the single-spike electrode could successfully penetrate the cell membrane. The force required to penetrate the cytoplasm membrane is known from AFM tips to be 10–30 nN.[31] If the tip size is further miniaturized, even a force of several hundred pN is sufficient to penetrate the membrane. The dielectrophoretic force acting on a cell located close to the single-spike electrode tip is calculated to be in the range of 0.05–1 μN at a voltage amplitude and frequency of 30 V_{pp} and 2 MHz, respectively, assuming typical cell parameters ($C_m = 0.7\ \mu F/cm^2$; spherical shape; radius = 10 μm; conductivity of cytoplasm = 3 mS/cm; permittivity = 100 F/m).[32,33] It has to be taken into account that there is a further force acting contrary to F_{DEP}, the drag force. However, drag force calculation according to the Stokes law[34] reveals a value of just 1 nN for a cell in DEP medium; thus, it is comparably small. Also, other aspects like gravitation or Brownian force may be neglected, as they play only a minor role during cell acceleration and/or penetration. The sharp electrode geometry is very important for a high penetration probability for several reasons. First, as can be concluded from *Equation (1)*, the dielectrophoretic force acting on a cell rises with the square of the electric field,[21] and thus is very strong close to the electrode tip (see also *Fig. 1B*). Second, the force necessary for the penetration decreases with a decreasing tip diameter, because the affected membrane area is smaller. In general, the measuring regime was established > 5 min after introducing cells to the chamber. Note that in an automated system based on microfluidic channels, the same process can be decreased to a few seconds using an electronic switch changing from DEP to potential measurement.

Nevertheless, the yield of penetrated cells was low. Essentially, this was due to the fact that cells have been distracted from the course of the attraction, mainly caused by a vertical drift (cell sedimentation). As a consequence, the distracted cells were prevented from perforation, because they were guided to the electrode base/taper instead of being impaled by the electrode tip (*Supplementary Fig. S3*), and once cells or cell compounds stacked at the electrode surface, successful impalement of a second cell was also prevented. In general, we were able to decrease the cell sedimentation by enhancing the density of the DEP medium by use of Nycodenz, which is also suitable in high–field-frequency experiments.[35,36] Nevertheless, we expect that these problems will be drastically reduced in an automated high-throughput system. As the single-spike microfluidic chamber was designed for microscopic control, a vertical carrier position was required. In contrast, in a high-throughput device, the working electrode would be placed on a plane surface, and thus sedimentation would not negatively affect the cell attraction. Also, by choosing an appropriate chamber design, cell positioning can become arbitrary; for example, the insulator design could be adapted such that lateral attachment of the cell to the electrode surface is hampered by appropriate structures (*Supplementary Fig. S3*). In some experiments, we observed convections known as jet streams[37,38] affecting the positioning of cells. Jet streams occur when conductivity of the cell suspension is too high and the medium is locally warmed due to the high electric-field intensity, causing cells to be rejected away from the single-spike electrode (*Supplementary Fig. S3*). In high-throughput systems, these effects can be eliminated by a decreased chamber volume with optimized solution exchange. In single-spike experiments, the distraction problems were circumvented by attraction of cell groups of 10–15 cells (multi-cell attraction) instead of just one single cell (single-cell attraction). The advantage was an enlarged electrode surface of the single-spike electrode (from ∼15 to ∼40 μm) accompanied by both, a decrease in the access resistance and an increase of potential stability. However, cells attracted by the multi-cell attraction technique could not be mechanically penetrated by the single-spike tip and had to be perforated by a series of square pulses to reveal intracellular contact.

In contrast to other electrophysiological methods in DAIMM, cells are required to be suspended in a low-conducting medium before establishment of the measurement regime. That is, before electromanipulation of cells, they have to be washed and suspended in a medium with ion concentration in the submillimolar range. As the Clausius-Mosotti factor [see *Eq. (1)*] is influenced by the frequency-dependent permittivity and conductivity of the medium and cell, respectively, the cell velocity is significantly lowered if the conductivity of the cell suspension is high. Furthermore, a lowered osmolarity of the DEP medium (200 mOsm) is required for successful membrane perforation. Under iso-osmolaric conditions, HEK293 cells exhibit membrane invaginations, whereas when they are exposed to a hypo-osmolaric medium, the membrane will be stretched and the cytoskeleton will decompose. Even though HEK293 cells show a slight regulatory volume decrease at 200 mOsm,[24] osmolarity was not further lowered to ensure good cell viability. One may argue that the exposition of cells to a low-ionic medium and electric fields could negatively influence the cell function. However, similar conditions have been used in several standard cell culture protocols for the last three decades.[19,21] Furthermore, we could recently show that membrane protein behavior remained unchanged after exposition of ChR2-expressing eukaryotic cells to electric fields.[24,39]

After establishment of the measurement array by dielectrophoretic attraction, the resistance increased from 1–50 MΩ (electrode resistance) to 0.3–0.8 GΩ. It has to be emphasized that the epoxy resin used for insulation of the single-spike electrode is chemically inert and is an excellent electrical insulator.[40] However, no sealing

between the epoxy resin and membranes was observed; thus it was necessary to isolate the electrode–solution interface by liposomes. Similarly to other devices based on the planar patch-clamp technique, the seal resistance measurement (also by impedance spectroscopy) could offer a standard output to gauge cell health.[41]

In an automated system, however, the insulating matrix should exhibit good sealing properties. As known from the patch-clamp techniques, it would be desirable that the polymer behaves similarly to glass, so that a high seal resistance between cell membrane and polymer is facilitated, as it is known from Orcomer® or polydimethylsiloxane.[42,43] High seal resistances are more important in voltage-clamp experiments, but a system based on the DAIMM method is not suitable to clamp the membrane potential, because the metal electrode exhibits a strong polarization in the contact surface between electrode and solution.[27,28,44] The layer of oppositely-charged ions alongside the surface behaves as a strong capacitor, with a magnitude of 0.1–10 mF/cm^2 (10 Hz).[23] For high-quality measurements, it is necessary to keep the electrode impedance as low as possible.[45] Indeed, series resistances of single-spikes used in DAIMM measurements ranged between 1 and 50 MΩ. Compared to other metals, at low frequencies, chlorinated silver electrodes combine low impedance and very high stability of the electrical potential of even the smallest electrodes (0.31 ± 0.33 mV). Typically, after cell impalement, the recorded potential was stable for >15 min and negatively shifted compared to that of the cell-free electrode in 100 mM NaCl. This potential change is not put on the same level as the membrane potential, since it also contains the electrode-potential change due to change of the chloride concentration, which could not be systematically evaluated with our model system.

We recorded light-induced changes in the membrane potential of HEK293 cells expressing ChR2[24,46] in a side-by-side study of patch-clamp (*Fig. 3A*) and DAIMM (*Fig. 3B*) method, respectively. In patch-clamp measurements, the membrane potential was depolarized upon blue-light illumination (473 nm), showing a characteristic transient peak followed by a stationary potential. Similarly, in DAIMM experiments, light-induced depolarization of the membrane potential of up to 25 mV was observed (*Fig. 3B*), but the transient peak was absent (three independent single-spike electrodes). The light-induced depolarization was repeated several times in every measurement. Note that a relatively low light-intensity was used in DAIMM experiments (HBO lamp <2 mW/mm^2), because the design of the chamber did not allow coupling a laser source into the system. It is well known from ChR2 that when the light intensity is low, the transient peak current disappears.[47] Besides that, the overall time resolution of the single-spike electrode was lower than that of the patch-clamp electrode (for details, see *Supplementary Fig. S4*).

Silver chloride is light sensitive,[48,49] and the electrode potential changes upon illumination (Bequerel effect).[50] Indeed, the silver chloride single-spike electrode responded to illumination by blue light with a slight potential change (*Fig. 3B*, lower trace; 1.02 ± 2.68 mV; see the Materials and Methods section), but the amplitude was at least one order of magnitude lower than ChR2-mediated membrane-potential changes and tended to show a slight hyperpolarization. However, DAIMM of control HEK293 cells without ChR2 expression illumination did not reveal any significant potential changes (*Fig. 3B*).

Due to the challenging and time-consuming manual manufacture process (one carrier in 20 min), it is inappropriate to use the single-spike–model electrode in high-throughput systems. Instead, microelectrodes with a symmetrical and reproducible electrode geometry are required to avoid any asymmetry of the electric field. For optimal penetration of the membrane, the electrode should be as thin as

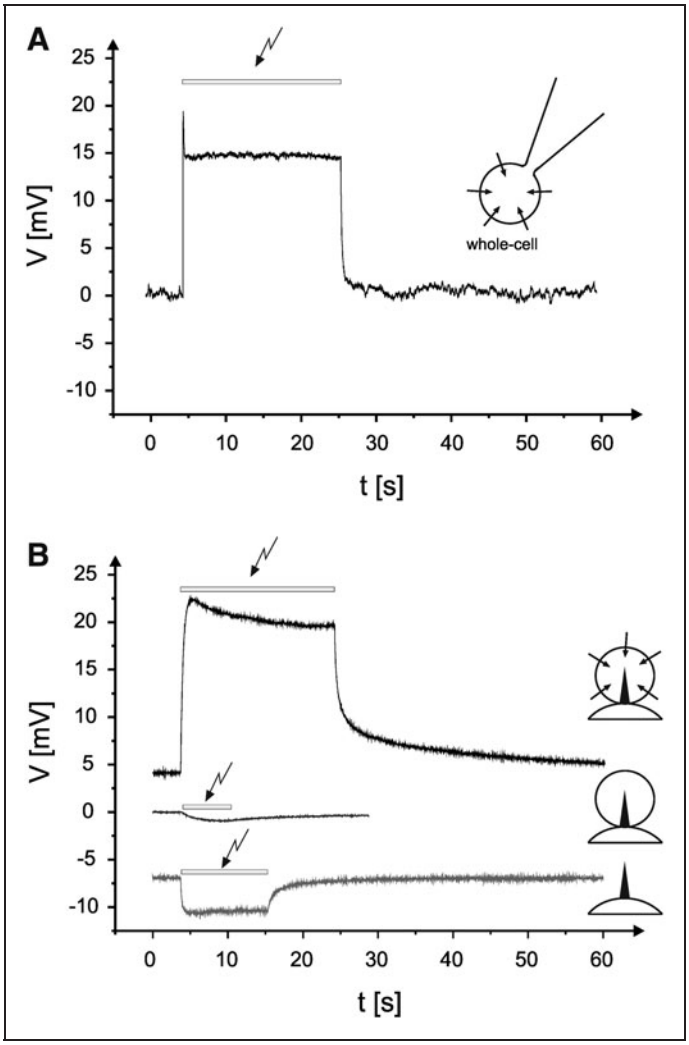

Fig. 3. Comparative measurements on HEK293 cells expressing ChR-2 with the DAIMM and the patch-clamp method. **(A)** A typical zero-current clamp measurement using the patch-clamp technique on a ChR2-expressing cell is shown. Note that during blue-light illumination (indicated by the arrow), a steady-state depolarization of the cell with an initial transient potential component occurs.[46] **(B)** Measurements by means of the DAIMM method using comparable experimental conditions as in **(A)**. The three voltage curves represent typical results in absence or presence of blue-light illumination experiments under zero-current clamp conditions by using HEK293 cells expressing ChR2, control HEK293 cells, and in the absence of any cells (*insets*).

possible, but on the other hand, for electrical reasons, a sharp tip (DEP) and extended electrode surface (potential measurement) are valuable. Metal microelectrodes with a geometrical form fulfilling both requirements may be produced by galvanic deposition of metal in a template, such as in ion-track etched polycarbonate films, or in 3D forms designed for photoresistance by two-photon polymerization (2PP).[51–53] We expect that findings from the single-spike electrode can be transferred to smaller electrodes, because micro- and nanometal electrodes show comparable miniaturization effects.[54]

In general, the DAIMM method has some strong advantages, which demonstrate its potential not only in the high-throughput screening for medically relevant substances, but also in environmental analytics. First, the dielectrophoretic force used for cell manipulation allows maintenance of even low cell concentrations, which is not the case with many planar patch-clamp systems requiring a high amount of cells to collect and place cells on the holes by low pressure.[6] Secondly, due to the fact that dielectrophoretic cell manipulation is applicable to low cell densities,[55] the benefit of the DAIMM method in pharmacological characterization of native cell probes, such as pathogenic tissue of patients, is very probable. Thirdly and most importantly, using the new DAIMM method, the cytoplasm does not need to be substituted by artificial solutions. This may enable electrophysiological measurements under more physiological conditions than in many high-throughput systems based on the planar patch-clamp method.[6,9,10] However, the new technique cannot supersede patch-clamp measurements, since the intracellular conditions are not defined and the membrane potential cannot be clamped by the metal electrode. Yet, taking all facts into account, the DAIMM method offers a good opportunity to analyze the interaction of compounds with cell types or ion channels in high-throughput systems. We expect that successful concepts of the high-throughput technology, like population patch-clamp (several electrodes are interrogated in one experiment, and data points are pooled) and dynaflow (the electrode is placed in a platform with many fluid channels for compound supplementation), can be transferred to the DAIMM technology.[11,56] Furthermore, the microdesign of the system would also allow combining the DAIMM method with cell sorting[57–60] and/or microcell fusion,[61–65] making further cell types accessible to high-throughput electrophysiology, for example, by enlarging yeasts[39] which are ideal candidates not only in channelopathy[66] but also for sensing environmental conditions.[67] Finally, we would like to mention that dielectrophoretic cell attraction may also be included in high-throughput systems based on the planar patch-clamp method by simply inserting a metal microelectrode in each hole.

ACKNOWLEDGMENTS

We thank Prof. E. Bamberg (MPI of Biophyics Frankfurt) and Prof. U. Zimmermann (University Würzburg) for valuable discussions; J. Reichert (MPI of Biophysics) for computer-aided design and construction of the 3D-chamber and *Figure 2*; A. Gessner and M. Behringer (University Würzburg) for construction of carrier blanks; R. Bergbauer and V. Friedmann for the design of the amplitude generator; and A. Pustlauck for excellent technical support. This work was supported by a grant to Prof. E. Bamberg, Dr. Habil. D. Zimmermann, and Prof. U. Zimmermann by BMBF Biochance Plus (0313369B).

DISCLOSURE STATEMENT

No competing financial interests exist.

REFERENCES

1. Bernard G, Shevell MI: Channelopathies: a review. *Pediatr Neurol* 2008;38:73–85.
2. Hübner CA, Jentsch TJ: Ion channel diseases. *Hum Mol Genet* 2002;11:2435–2445.
3. Camerino DC, Tricarico D, Desaphy JF: Ion channel pharmacology. *Neurotherapeutics* 2007;4:184–198.
4. Overington JP, Al-Lazikani B, Hopkins AL: Opinion–how many drug targets are there? *Nature Rev Drug Discov* 2006;5:993–996.
5. Chen Y, Zhong JF: Microfluidic devices for high-throughput gene expression profiling of single hESC-derived neural stem cells. *Methods Mol Biol* 2008;438:293–303.
6. Dunlop J, Bowlby M, Peri R, Vasilyev D, Arias R: High-throughput electrophysiology: an emerging paradigm for ion-channel screening and physiology. *Nat Rev Drug Discov* 2008;7:358–368.
7. Sigworth FJ, Klemic KG: Patch clamp on a chip. *Biophys J* 2002;82:2831–2832.
8. Willumsen NJ, Bech M, Olesen SP, Jensen BS, Korsgaard MPG, Christophersen P: High throughput electrophysiology: new perspectives for ion channel drug discovery. *Recept Channel* 2003;9:3–12.
9. Stoelzle S: State-of-the-art automated patch clamp devices: heat activation, action potentials, and high throughput in ion channel screening. *Front Pharmacol* 2011;2:76.
10. Stava E, Yu M, Shin HC, Shin H, Rodriguez J, Blick RH: Mechanical actuation of ion channels using a piezoelectric planar patch clamp system. *Lab Chip* 2012;12:80–87.
11. Möller C, Slack M: Impact of new technologies for cellular screening along the drug value chain. *Drug Discov Today* 2010;15:384–390.
12. Sarantopoulos C: Perforated patch-clamp techniques. *Neuromethods* 2007;38:253–293.
13. Pusch M, Neher E: Rates of diffusional exchange between small cells and a measuring patch pipette. *Pflugers Arch* 1988;411:204–211.
14. Natarajan A, Molnar P, Sieverdes K, Jamshidi A, Hickman JJ: Microelectrode array recordings of cardiac action potentials as a high throughput method to evaluate pesticide toxicity. *Toxicol In Vitro* 2006;20:375–381.
15. Nam Y, Wheeler BC: *In vitro* microelectrode array technology and neural recordings. *Crit Rev Biomed Eng* 2011;39:45–61.
16. Stett A, Egert U, Guenther E, *et al.*: Biological application of microelectrode arrays in drug discovery and basic research. *Anal Bioanal Chem* 2003;377:486–495.
17. Hanein Y: Towards MEMS probes for intracellular recording. *Sensors Update* 2002;10:47–75.
18. Xie C, Lin Z, Hanson L, Cui Y, Cui B: Intracellular recording of action potentials by nanopillar electroporation. *Nat Nanotechnol* 2012;7:185–190.
19. Dimitrov DS: Electroporation and electrofusion of membranes. In: *Handbook of Biological Physics–Structure and Dynamics of Membranes.* Lipowsky R, Sackmann E (eds.), pp. 851–900, Elsevier, Amsterdam, 1995.
20. Jones TB: Basic theory of dielectrophoresis and electrorotation. *IEEE Eng Med Biol Mag* 2003;22:33–42.
21. Zimmermann U, Neil GA, eds.: *Electromanipulation of Cells.* CRC Press, New York, 1996.
22. Khoshmanesh K, Nahavandi S, Baratchi S, Mitchell A, Kalantar-zadeh K: Dielectrophoretic platforms for bio-microfluidic systems. *Biosens Bioelectron* 2011;26:1800–1814.
23. Geddes LA: *Electrodes and the Measurement of Bioelectric Events.* Willey Interscience, New York, 1972.
24. Zimmermann D, Terpitz U, Zhou A, *et al.*: Biophysical characterisation of electrofused giant HEK293-cells as a novel electrophysiological expression system. *Biochem Biophys Res Commun* 2006;348:673–681.

25. Iwami M, Uehara Y, Ushioda S: Preparation of silver tips for scanning tunneling microscopy imaging. *Rev Sci Instrum* 1998;69:4010–4011.
26. Melmed AJ: The art and science and other aspects of making sharp tips. *J Vac Sci Technol B* 1991;9:601–608.
27. Gesteland RC, Howland B, Lettvin JY, Pitts WH: Comments on microelectrodes. *Proc IRE* 1959;47:1856–1862.
28. Geddes LA, Roeder R: Measurement of the direct-current (Faradic) resistance of the electrode-electrolyte interface for commonly used electrode materials. *Ann Biomed Eng* 2001;29:181–186.
29. Getzel WA, Webster JG: Minimizing silver-silver chloride electrode impedance. *IEEE Trans Biomed Eng* 1976;23:87–88.
30. Wiegand G, Arribas-Layton N, Hillebrandt H, Sackmann E, Wagner P: Electrical properties of supported lipid bilayer membranes. *J Phys Chem* 2002;106:4245–4254.
31. Hategan A, Law R, Kahn S, Discher DE: Adhesively-tensed cell membranes: lysis kinetics and atomic force microscopy probing. *Biophys J* 2003;85:2746–2759.
32. Zimmermann D, Zhou A, Kiesel M, *et al.*: Effects on capacitance by overexpression of membrane proteins. *Biochem Biophys Res Commun* 2008;369:1022–1026.
33. Markx GH, Davey CL: The dielectric properties of biological cells at radiofrequencies: applications in biotechnology. *Enzyme Microb Technol* 1999;25:161–171.
34. Du F, Baune M, Thoming J: Insulator-based dielectrophoresis in viscous media—simulation of particle and droplet velocity. *J Electrostat* 2007;65:452–458.
35. Arnold WM, Gessner AG, Zimmermann U: Dielectric measurements on electro-manipulation media. *Biochim Biophys Acta* 1993;1157:32–44.
36. Rickwood D, Ford T, Graham J: Nycodenz—a new nonionic iodinated gradient medium. *Anal Biochem* 1982;123:23–31.
37. Green NG, Ramos A, Gonzalez A, Morgan H, Castellanos A: Fluid flow induced by nonuniform ac electric fields in electrolytes on microelectrodes. I. Experimental measurements. *Phys Rev E* 2000;61:4011–4018.
38. Sitte B, Rath HJ: Influence of the dielectrophoretic force on thermal convection. *Exp Fluids* 2003;34:24–27.
39. Terpitz U, Raimunda D, Westhoff M, *et al.*: Electrofused giant protoplasts of *Saccharomyces cerevisiae* as a novel system for electrophysiological studies on membrane proteins. *Biochim Biophys Acta* 2008;1778:1493–1500.
40. Gaw KO, Kakimoto M: Polyimide-epoxy composites. *Adv Polym Sci* 1999;140:107–136.
41. Pathak P, Zhao H, Gong Z, *et al.*: Real-time monitoring of cell viability using direct electrical measurement with a patch-clamp microchip. *Biomed Microdevices* 2011;13:949–953.
42. Pantoja R, Nagarah JM, Starace DM, *et al.*: Silicon chip-based patch-clamp electrodes integrated with PDMS microfluidics. *Biosens Bioelectron* 2004;20:509–517.
43. Schlie S, Ngezahayo A, Ovsianikov A, *et al.*: Three-dimensional cell growth on structures fabricated from ORMOCER (R) by two-photon polymerization technique. *J Biomater Appl* 2007;22:275–287.
44. Ritchie IM, Bailey S, Woods R: The metal-solution interface. *Adv Colloid Interface Sci* 1999;80:183–231.
45. Zhou H, Tilton RD, White LR: The role of electrode impedance and electrode geometry in the design of microelectrode systems. *J Colloid Interface Sci* 2006;297:819–831.
46. Nagel G, Szellas T, Huhn W, *et al.*: Channelrhodopsin-2, a directly light-gated cation-selective membrane channel. *Proc Nat Acad Sci USA* 2003;100:13940–13945.
47. Hegemann P, Ehlenbeck S, Gradmann D: Multiple photocycles of channelrhodopsin. *Biophys J* 2005;89:3911–3918.
48. Aline PG: Optical and electrical properties of silver chloride. *Phys Rev* 1957;105:406–412.
49. Lanz M, Schurch D, Calzaferri G: Photocatalytic oxidation of water to O-2 on AgCl-coated electrodes. *J Photochem Photobiol A* 1999;120:105–117.
50. Schurch D, Currao A, Sarkar S, Hodes G, Calzaferri G: The silver chloride photoanode in photoelectrochemical water splitting. *J Phys Chem B* 2002;106:12764–12775.
51. Ostendorf A, Chichkov BN: Two-photon polymerization: a new approach to micromachining. *Photonics Spectra* 2006;40:72–81.
52. Passinger S, Stepanov A, Evlyukhin A, Reinhardt C, Kiyan R, Chichkov B: Two-photon polymerization and applications in plasmonics. *Proc SPIE* 2007;6581:U1–U8.
53. Wu SH, Serbin J, Gu M: Two-photon polymerisation for three-dimensional micro-fabrication. *J Photochem Photobiol A* 2006;181:1–11.
54. Forster RJ: Microelectrodes—new dimensions in electrochemistry. *Chem Soc Rev* 1994;23:289–297.
55. Gagnon ZR: Cellular dielectrophoresis: applications to the characterization, manipulation, separation and patterning of cells. *Electrophoresis* 2011;32:2466–2487.
56. Southan A, Clark G: Recent advances in electrophysiology-based screening technology and the impact upon ion channel discovery research. *Methods Mol Biol* 2009;565:187–208.
57. Kang YJ, Li DQ, Kalams SA, Eid JE: DC-dielectrophoretic separation of biological cells by size. *Biomed Microdevices* 2008;10:243–249.
58. Kralj JG, Lis MTW, Schmidt MA, Jensen KF: Continuous dielectrophoretic size-based particle sorting. *Anal Chem* 2006;78:5019–5025.
59. Graham DM, Messerli MA, Pethig R: Spatial manipulation of cells and organelles using single electrode dielectrophoresis. *BioTechniques* 2012;52:39–43.
60. Ma W, Shi T, Tang Z, Liu S, Malik R, Zhang L: High-throughput dielectrophoretic manipulation of bioparticles within fluids through biocompatible three-dimensional microelectrode array. *Electrophoresis* 2011;32:494–505.
61. Chiu DT: A microfluidics platform for cell fusion—commentary. *Curr Opin Chem Biol* 2001;5:609–612.
62. Skelley AM, Kirak O, Suh H, Jaenisch R, Voldman J: Microfluidic control of cell pairing and fusion. *Nat Methods* 2009;6:147–152.
63. Kemna EWM, Wolbers F, Vermes I, van den Berg A: On chip electrofusion of single human B cells and mouse myeloma cells for efficient hybridoma generation. *Electrophoresis* 2011;32:3138–3146.
64. Hu N, Yang J, Yin Z-Q, *et al.*: A high-throughput dielectrophoresis-based cell electrofusion microfluidic device. *Electrophoresis* 2011;32:2488–2495.
65. Kirschbaum M, Guernth-Marschner CR, Cherré S, *et al.*: Highly controlled electrofusion of individually selected cells in dielectrophoretic field cages. *Lab Chip* 2012;12:443–450.
66. Wolfe DM, Pearce DA: Channeling studies in yeast—yeast as a model for channelopathies? *Neuromol Med* 2006;8:279–306.
67. Baronian KHR. The use of yeast and moulds as sensing elements in biosensors. *Biosens Bioelectron* 2004;19:953–962.

Address correspondence to:
Ulrich Terpitz, PhD
Department of Biotechnology and Biophysics
Julius–Maximilians University Würzburg
Biocenter/Am Hubland
D-97074 Würzburg
Germany

E-mail: ulrich.terpitz@uni-wuerzburg.de